

# Structural designation and mechanical properties of TiNi/Ti2Ni laminated composites

C Jia<sup>1,2</sup>, Z P Xiong<sup>1,2\*</sup>, Z Liu<sup>1,2</sup> and X W Cheng<sup>1,2\*</sup>



<sup>1</sup>School of Materials Science and Engineering, Beijing Institute of Technology, Beijing 100081, P.R. China

<sup>2</sup>National Key Laboratory of Science and Technology on Materials under Shock and Impact, Beijing 100081, P.R. China

## Introduction

Laminated composite is developed on the basis of in-depth study of the microstructure and mechanical behavior of shell nacre. Laminated composite is generally formed by arranging two or more foils with different physical or chemical properties associated with certain layer spacing and layer thickness ratio. Because of small layer spacing and multi-interface effect, the performance of laminated composite is better than that of the corresponding monomer material.

Advanced composite armors have a front that deforms the projectile tip and, in turn, has the capability to reduce penetration when improving mechanical properties such as high hardness, thermal resistance, and compressive strength. Although these properties can be achieved by intermetallics alone, intermetallics cannot be used for armors on their own because of brittle fracture. On the other hand, ductile materials can provide structural integrity to prevent complete penetration of projectiles and absorb projectile energy.

## Aim

Fabricated inhomogeneous TiNi/Ti2Ni laminated composites using hot isostatic pressing (HIP) furnace and systematically investigated the effect of designed inhomogeneous structures on mechanical properties.

## Method

TiNi/Ti2Ni laminated composites were fabricated using hot isostatic pressing (HIP) furnace together with structural designation by the control of Ti and Ni foil thicknesses. Through adjusting the thickness ratio of Ti and Ni foils, the ratio of TiNi and Ti2Ni fraction can be controlled.

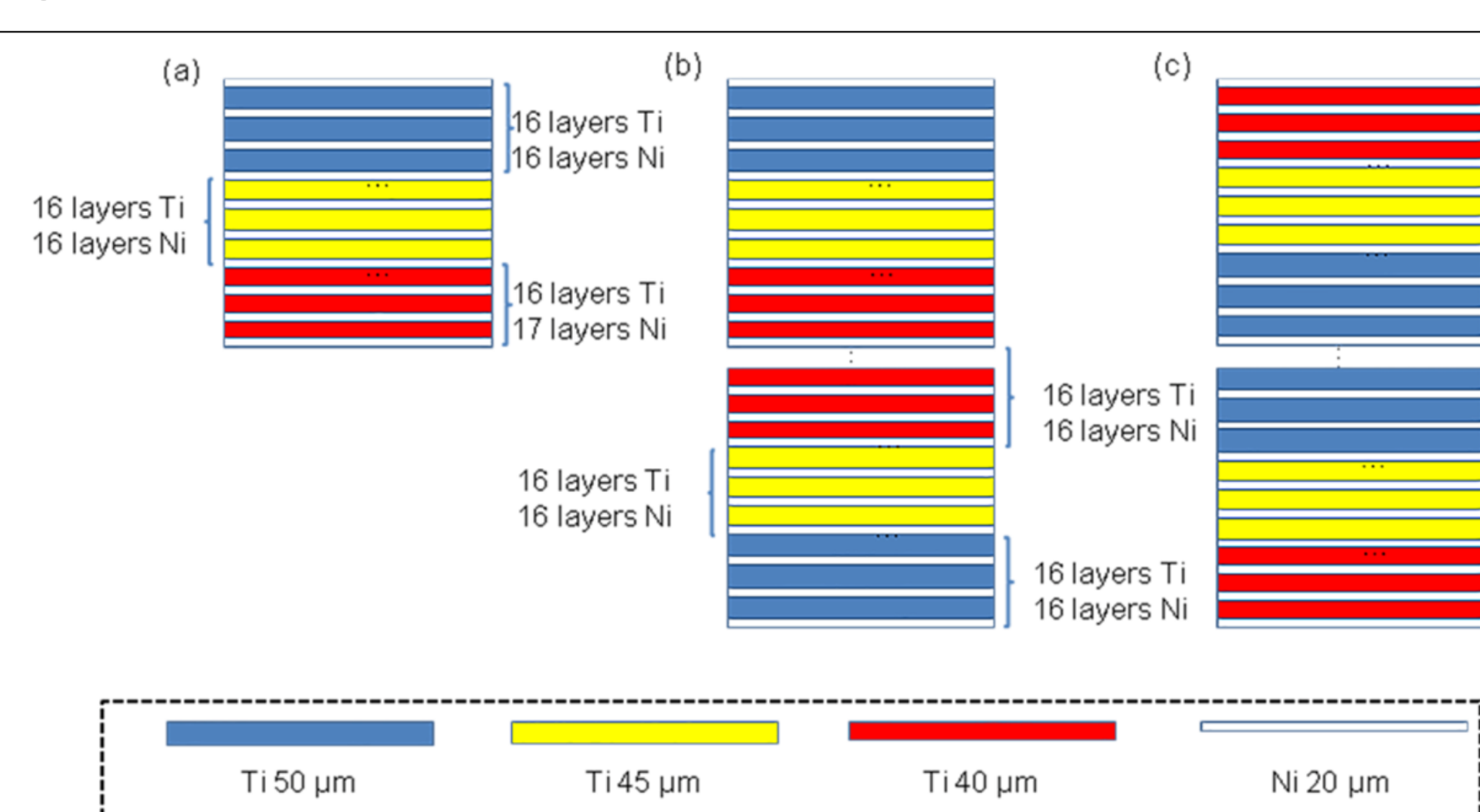
Microstructures were characterized using a scanning electron microscopy (SEM) equipped with a backscattered electron (BSE) detector.

The fracture toughness was measured by three-point bending (TPB) tests at room temperature.

Uniaxial compression tests were performed at room temperature and at a strain rate of  $1 \times 10^{-3} \text{ s}^{-1}$ .

Split-Hopkinson pressure bar (SHPB) was used to test the dynamic compressive properties.

All the loading direction was along the laminate thickness. Fracture surfaces were examined using SEM.

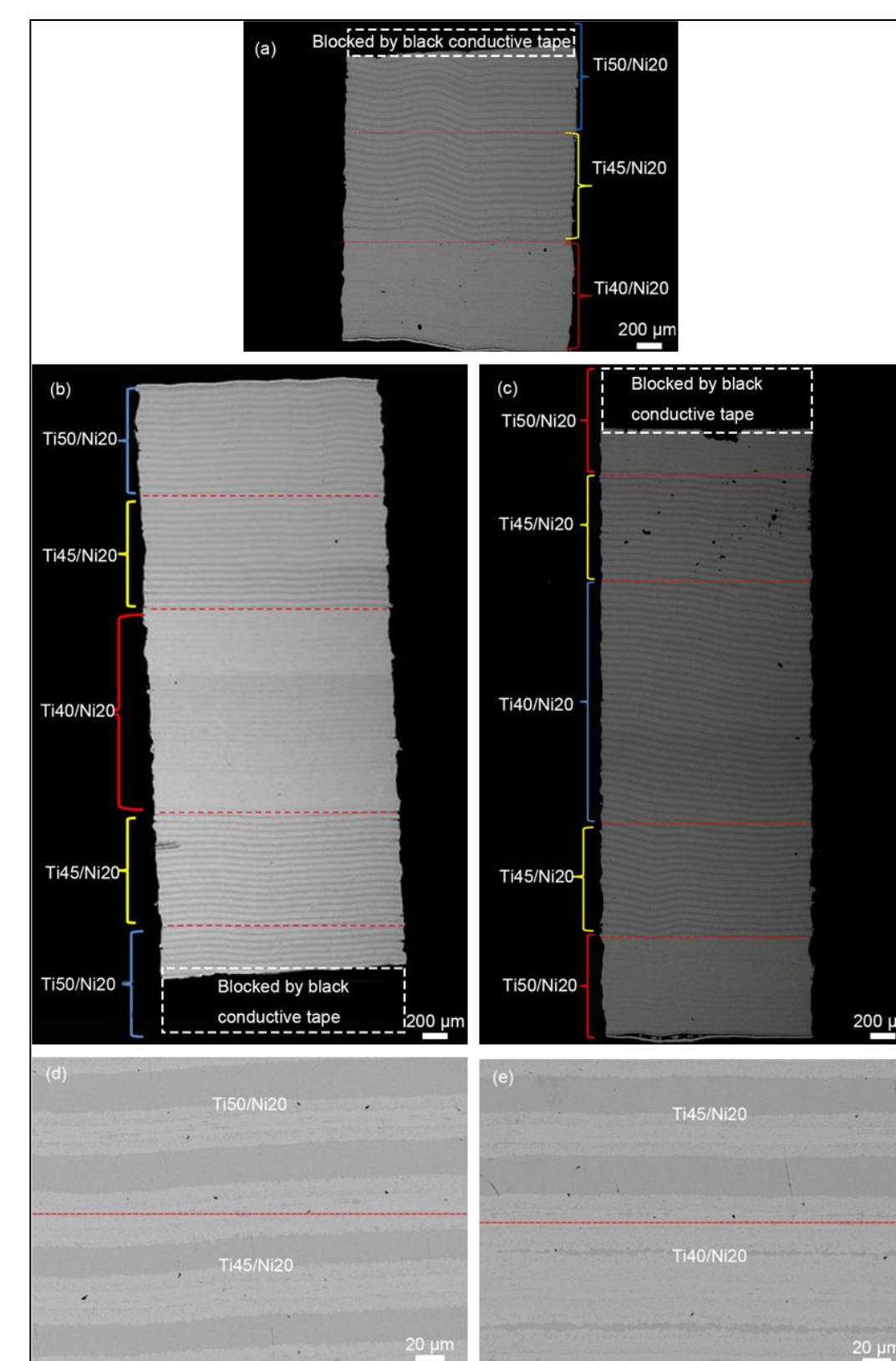


Schematic diagram of three stacking schemes.

## Results

Ti50/Ni20 layer is the hardest with high strength, while Ti40/Ni20 layer is the softest with good toughness. As a result, sample 1 exhibited hard-intermediate-soft laminated composites where hard, intermediate and soft layers were sintered by Ti50/Ni20, Ti45/Ni20 and Ti40/Ni20, respectively.

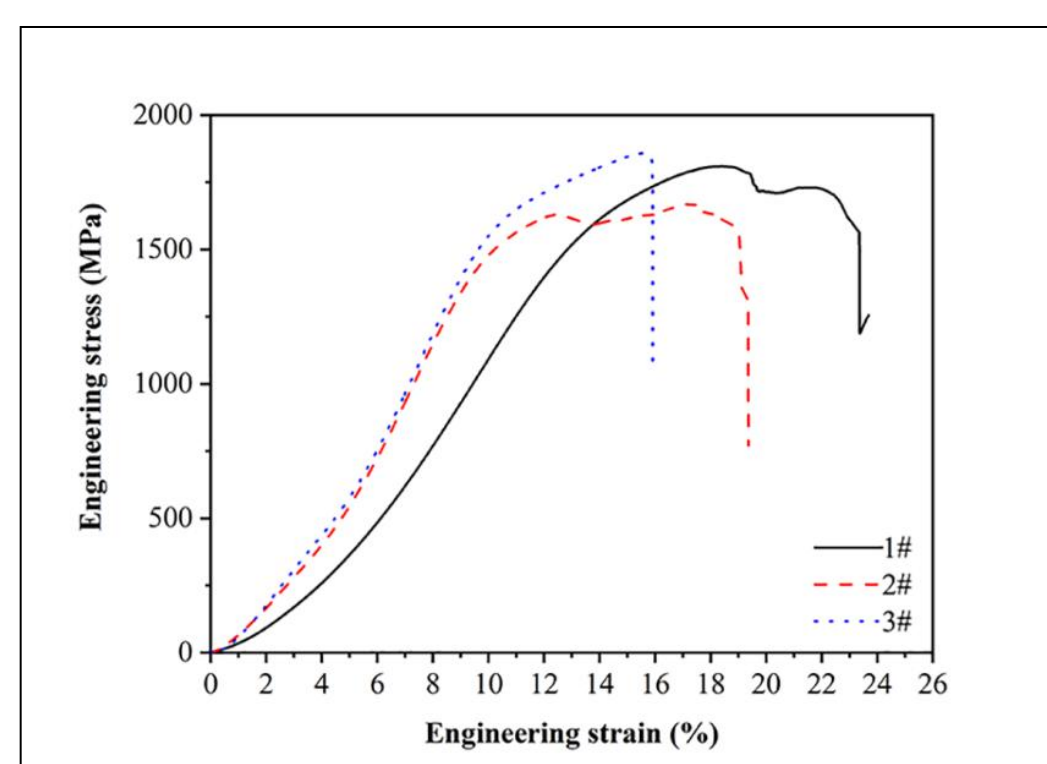
Sample 2 shows symmetrical gradient structure. This is called as soft-hard-soft structure. Sample 3 shows symmetrical gradient structure. This is named as hard-soft-hard structure.



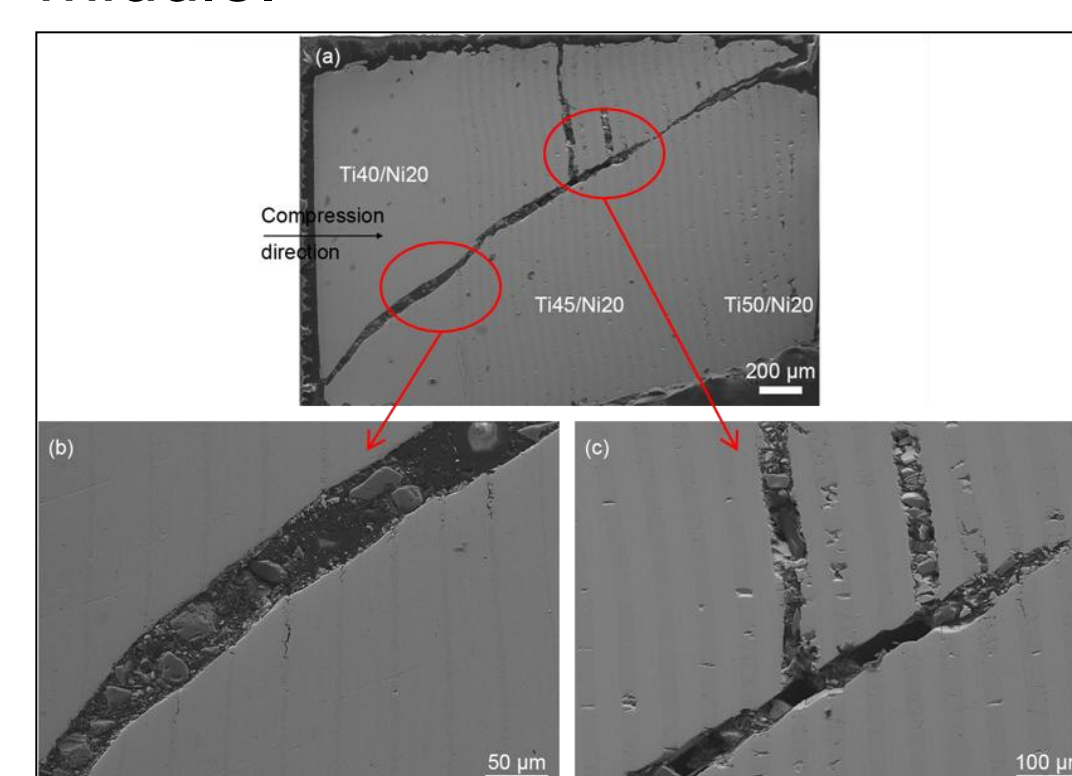
(a-c) Full view of (a) sample 1, (b) sample 3 and (c) sample 2 in BSE mode; (d, e) representative transition microstructures in sample 2 (d) from Ti50/Ni20 layer to Ti45/Ni20 layer and (e) from Ti45/Ni20 layer to Ti40/Ni20 layer.

The elastic modulus of sample 2 and sample 3 were basically the same, while that of sample 1 was relatively small.

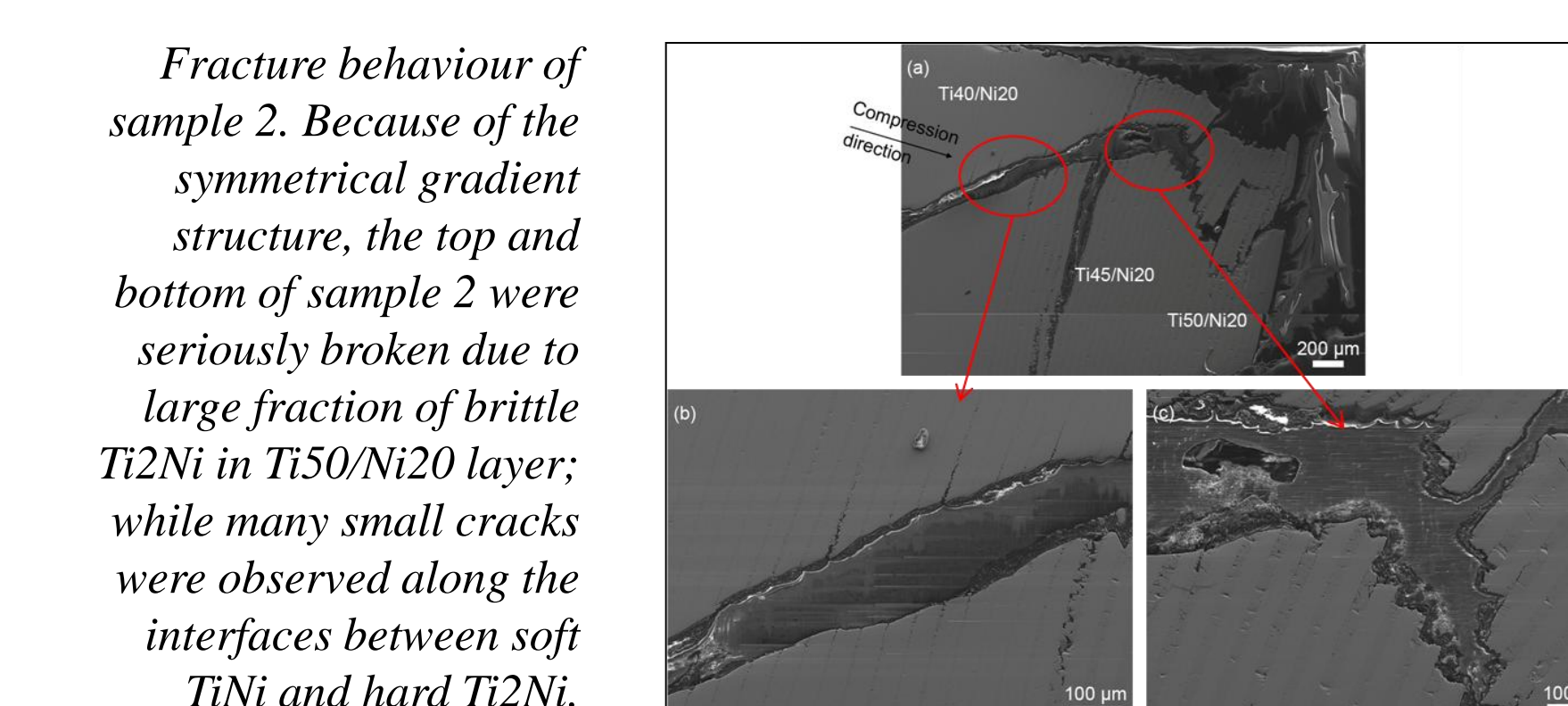
Compressive engineering stress-strain curves at static condition. The compressive strength of sample 3 is the highest ( $1853 \pm 4 \text{ MPa}$ ), while sample 2 has the smallest compressive strength ( $1690 \pm 20 \text{ MPa}$ ). The fracture strain of sample 1 was 23%, while sample 2 and sample 3 had fracture strain of 19% and 16%, respectively.



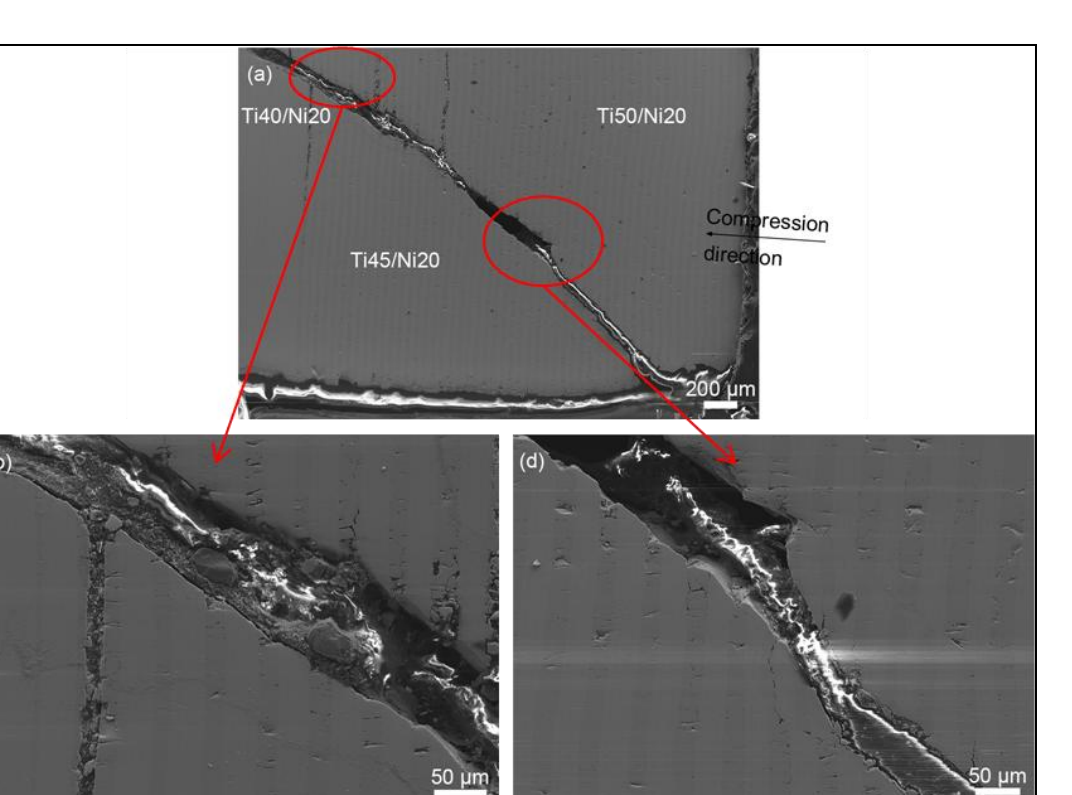
All three samples exhibited a typical main crack having an angle of  $45^\circ$  with compression direction due to the largest shear stress in this direction. The sample 3 was fracture earlier than sample 2 because harder parts of sample 3 were in the middle.



Fracture behaviour of sample 1. Many cracks were observed in Ti2Ni because it was brittle.



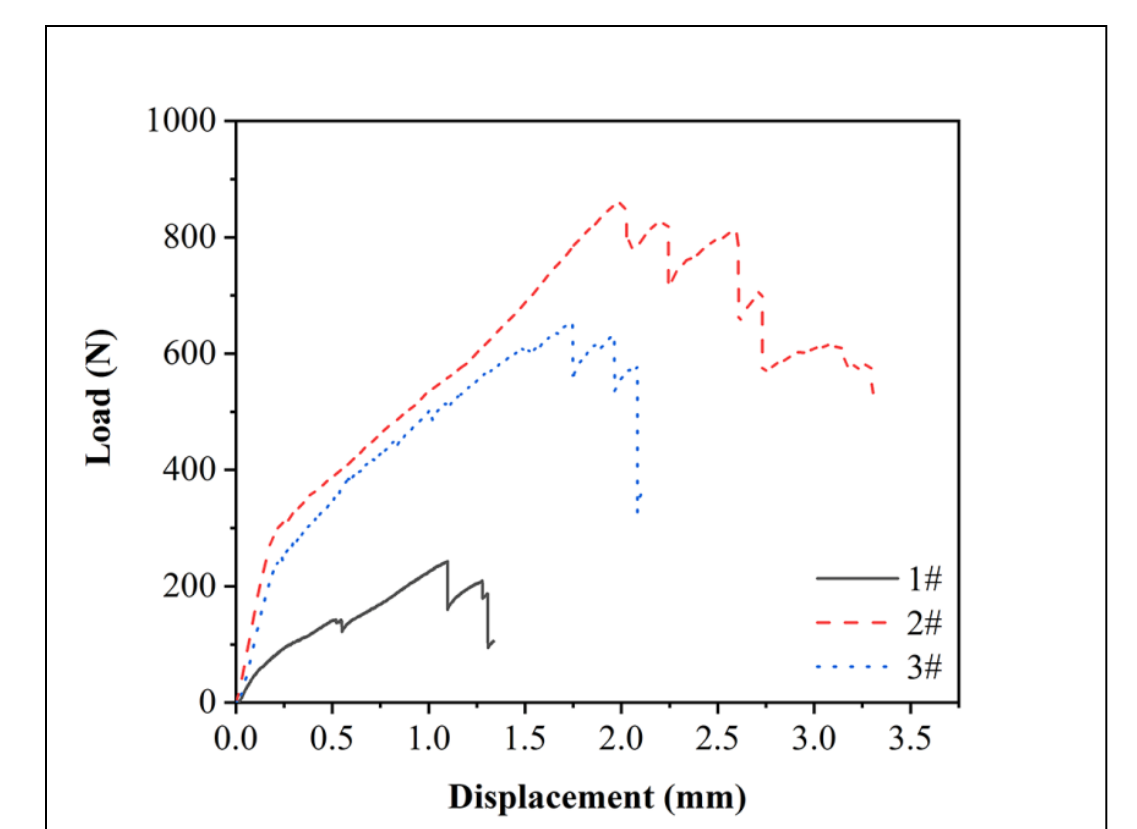
Fracture behaviour of sample 2. Because of the symmetrical gradient structure, the top and bottom of sample 2 were seriously broken due to large fraction of brittle Ti2Ni in Ti50/Ni20 layer; while many small cracks were observed along the interfaces between soft TiNi and hard Ti2Ni.



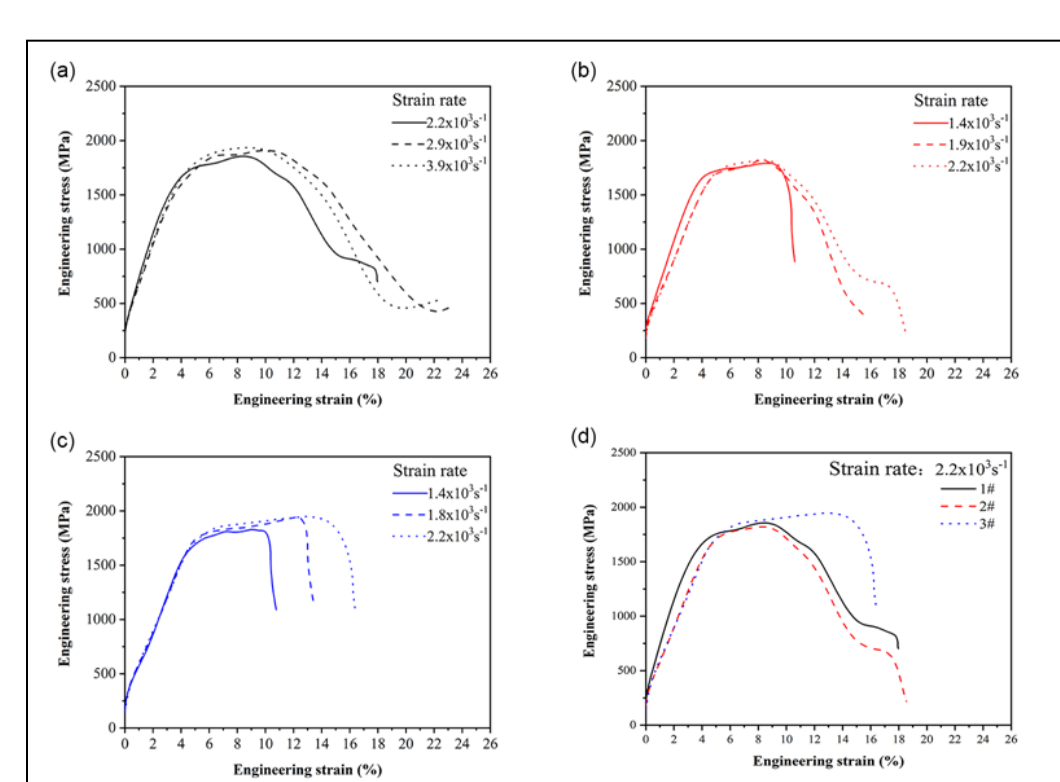
Fracture behaviour of sample 3. For sample 3, similar fracture behavior was observed, showing a main crack and many small cracks.

The thickness of ductile layer in the middle of sample 2 was the largest due to hard-soft-hard structure. This hindered the crack propagation and delayed the fracture, leading to the largest fracture toughness ( $37.9 \pm 2.7 \text{ MPa}\cdot\text{m}^{1/2}$ ) in comparison with sample 1 ( $27.2 \pm 5.1 \text{ MPa}\cdot\text{m}^{1/2}$ ) and sample 3 ( $30.6 \pm 1.8 \text{ MPa}\cdot\text{m}^{1/2}$ ).

Load-displacement curves of three-point bending tests.

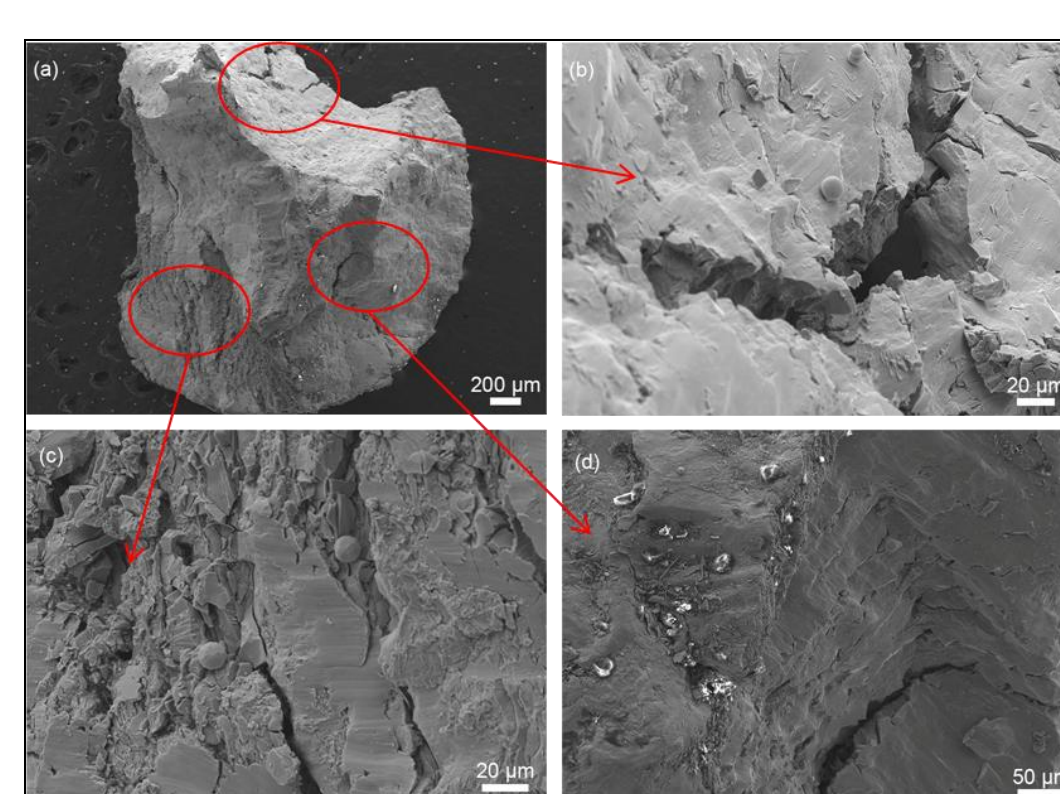


the compressive strength of sample 1 at strain rates of  $2.2 \times 10^3 \text{ s}^{-1}$ ,  $2.9 \times 10^3 \text{ s}^{-1}$  and  $3.9 \times 10^3 \text{ s}^{-1}$  were 1856 MPa, 1910 MPa and 1935 MPa respectively.

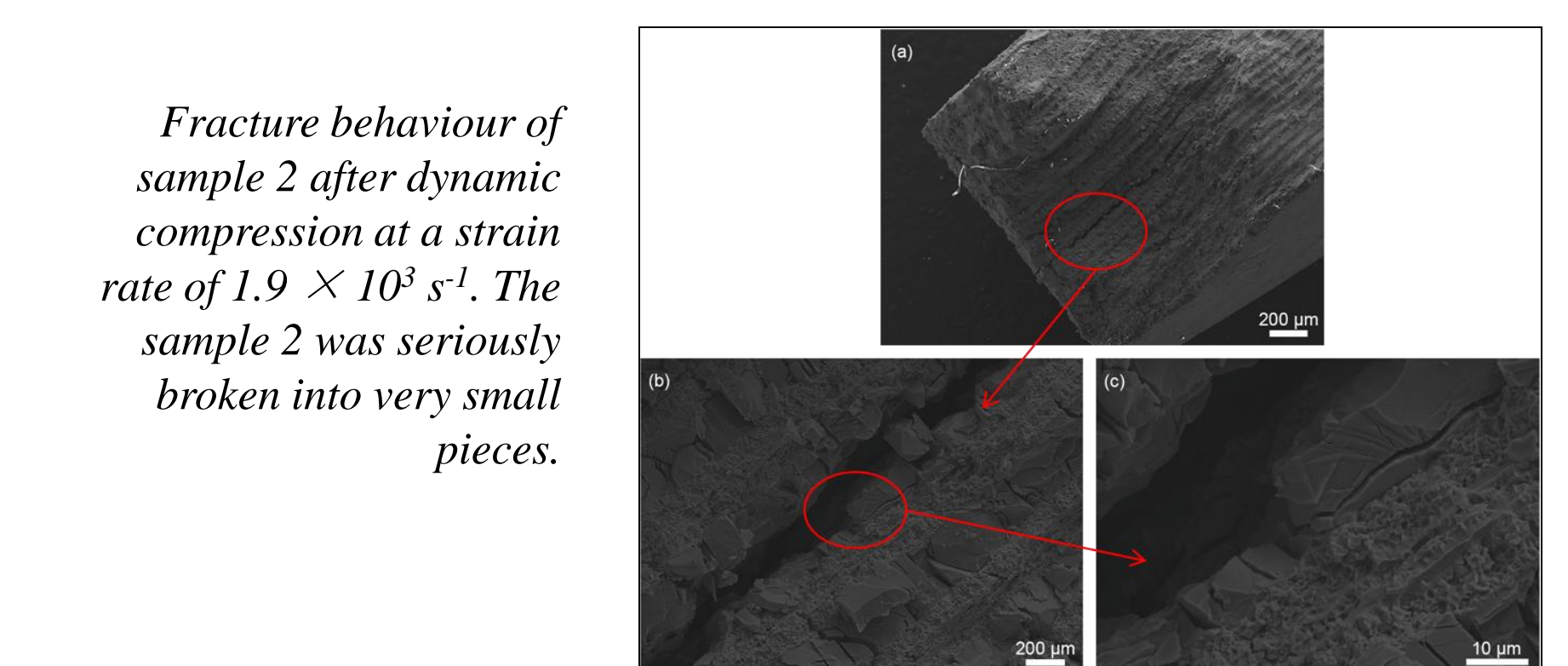


(a-c) Compressive engineering stress-strain curves at high strain rates of (a) sample 1, (b) sample 2 and (c) sample 3. (d) Compressive engineering stress-strain curves at a strain rate of  $2.2 \times 10^3 \text{ s}^{-1}$  for different structures.

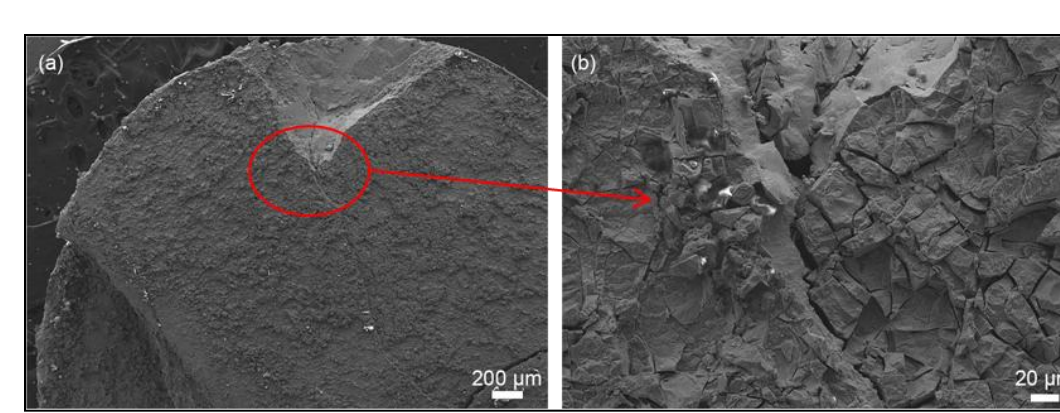
Interestingly, sample 3 had a relatively small degree of fragmentation and retained a relatively complete part of bottom. This fracture behavior was related to soft-hard-soft structure. Due to the top soft layer, it can be deformed and absorb energy. The middle layer was hard and also absorbed energy in the form of cracks and fragments. The bottom layer was soft and absorbed energy in the form of plastic deformation.



Fracture behaviour of sample 1 after dynamic compression at a strain rate of  $2.2 \times 10^3 \text{ s}^{-1}$ . A large number of cleavage steps and ductile shear tear cracks were observed in the sample 1.



Fracture behaviour of sample 2 after dynamic compression at a strain rate of  $1.9 \times 10^3 \text{ s}^{-1}$ . The sample 2 was seriously broken into very small pieces.



Fracture behaviour of sample 3 after dynamic compression at a strain rate of  $2.2 \times 10^3 \text{ s}^{-1}$ . sample 3 had a relatively small degree of fragmentation and retained a relatively complete part of bottom.

## Conclusion

(1) Through adjusting the thickness ratio of Ti and Ni foils, the ratio of TiNi and Ti2Ni fraction can be controlled. Hard-soft-hard, soft-hard-soft and hard-intermediate-soft laminated composites were designed.

(2) All three laminated composites had compression strength of 1690 ~ 1853 MPa and fracture toughness of  $27.2 \sim 37.9 \text{ MPa}\cdot\text{m}^{1/2}$  due to the same constituents of TiNi and Ti2Ni. However, the soft-hard-soft structure showed the best response under high strain rate because it was fractured into larger pieces while the other two structures were fractured into smaller pieces together with smaller fracture strain.

(3) This study demonstrated that the mechanical performance of laminated composites can be tuned by arranging soft layer and hard layer in different modes.